Samalas Journal of Geoenvironmental. Vol. 1 (1) **2025** | https://doi.org/10.59535/g8jpfm32

Research Paper

Analysis of Local Footprint Effects Due to the Lombok Earthquake in July-August 2018 in Labuapi District, West Lombok Regency

Hidayatul Islamiyah, Syamsuddin Syamsuddin *, Bakti Sukrisna

[1] Physics Study Program, Faculty of Mathematics and Natural Sciences, University of Mataram, **Indonesia**

* Correspondence: syamsuddin@unram.ac.id

This article contributes to:

Editor:
Safira Dwirizqia

Article Information:
Received: 21/04/25
Accepted: 26/04/25
Published: 28/04/25

Publisher's Note:
Futura Techno-Science stays neutral with regard to jurisdictional claims in published maps and institutional affiliations.

Abstract: Lombok island is one of the areas prone to earthquakes. In 2018 an earthquake occurred which caused most of the regions in Lombok to experience its effects, one of which was in Labuapi District. This study aims to analyze the characteristics of local footprint effects based on frequency and amplification values using the Horizontal to Vertical Spectral Ratio (HVSR) method and seismic vulnerability index (Kg), Vs30, and Peak Ground Acceleration (PGA) methods. The structure of the coating on the research area has a relatively low frequency value of 0.6 Hz – 12 Hz, with variations of amplification factors between 1 – 11. Seismic vulnerability index (Kg) variation ranges from 0.25 - 150, which illustrates the study area has a relatively high level of vulnerability. The Vs30 value in the study area was found to be relatively low at 240 m/s - 262 m/s, while the PGA values obtained ranged between 160 cm/s^2 -760 cm/s^2. By looking at the results of the correlation between measurement data with damage data that shows that damage to the study area is more dominantly influenced by building structures.

Keywords: Microtremor; HVSR; Seismic Vulnerability Index; Vs30; PGA.

1. Introduction

Lombok Island is one of the earthquake-prone areas. There are two earthquake source zones that increase the risk of earthquakes, the first is the Indo-Australian subduction zone in the south of West Nusa Tenggara and the second is the back arc thrust fault in the north of West Nusa Tenggara [1]. Based on historical earthquake data, Lombok Island has been rocked by an earthquake with a magnitude above 5 SR. [2]. The 6.9 SR earthquake that occurred in 2018 caused damage to parts of Lombok, one of which was in the Labuapi District. Labuapi District is located on alluvium deposits which are deposits of gravel, pebbles, sand, clay, and peat [3]. This shows that Labuapi District is very vulnerable to earthquakes because it is located on alluvium deposits which are deposits that are known to be soft and can enlarge (amplify) seismic waves from earthquakes so that they can strengthen the effects of earthquakes that come to this area. Based on field surveys in four villages in Labuapi District, the impact of damage caused by earthquakes in this area falls into the category of light damage to heavy damage as in Figure 1. Therefore, this study is very necessary to analyze the structure of soil layers in the Labuapi District area.

Measurements to determine the structure of the soil layer in this study used microtremors. Microtremors are natural harmonic vibrations of the soil that occur continuously which are produced by subsurface movements. To analyze natural vibrations of the soil (microtremors) is HVSR (Horizontal to Vertical Spectral Ratio) [4]. HVSR can be used to analyze natural vibrations in a certain area caused by local geological effects called site effects based on dominant frequency (f0), amplification factor (A0), seismic vulnerability index (Kg), sediment thickness (H), and Ground Shear Strain (GSS). From several parameters, an analysis can be made regarding earthquake-prone areas [5].

Site effect is a condition of the soil or subsurface under a building where damage has occurred to the soil structure on the surface [6]. Site effect is influenced by lithology and topography. Softer lithology tends to provide a long period of vibration response (low frequency) and has a higher risk when shaken by earthquake waves because it will experience greater amplification compared to more compact rocks [7]. Topographic effects that affect seismic response due to the amplification of ground motion around the peak and de-amplification around the foot of the slope. Large amplification factors are found not only

on hilltops but also on topographic slopes, while small amplification is found on steep slopes [8].

Table 1. History of Earthquakes in Lombok with Magnitude above 5 SR

No	Date	Coordinate		Depth (km)	Mag (SR)	The area that feels
		Lat	Long			
1	30/05/1979	-8,21	115,95	25	6.1	Lombok, Bali
2	01/01/2004	-8,34	115,87	33	6.1	Karangasem, Mataram, Lombok
3	22/06/2013	-8,43	116,04	10	5.4	Lombok, Kuta, Denpasar Gianyar, Karangasem
4	28/07/2018	-8,32	116,50	7	6.5	Lombok, Mataram, Sumbawa, Denpasar
4	29/07/2018	-8,4	116,5	24	6.5	Lombok, Mataram, Sumbawa, Denpasar
5	5/8/2018	-8,35	116,46	32	6.9	Lombok, Mataram, Bima, Bali, Banyuwangi
6	9/8/2018	-8,34	116, 22	9	5.8	Lombok, Mataram, Sumbawa
7	9/8/2018	-8,36	116,58	9	6.5	Lombok, Mataram, Sumbawa
8	19/8/2018	-8,30	116,66	9	6.8	Lombok, Denpasar, Makasar, Malang

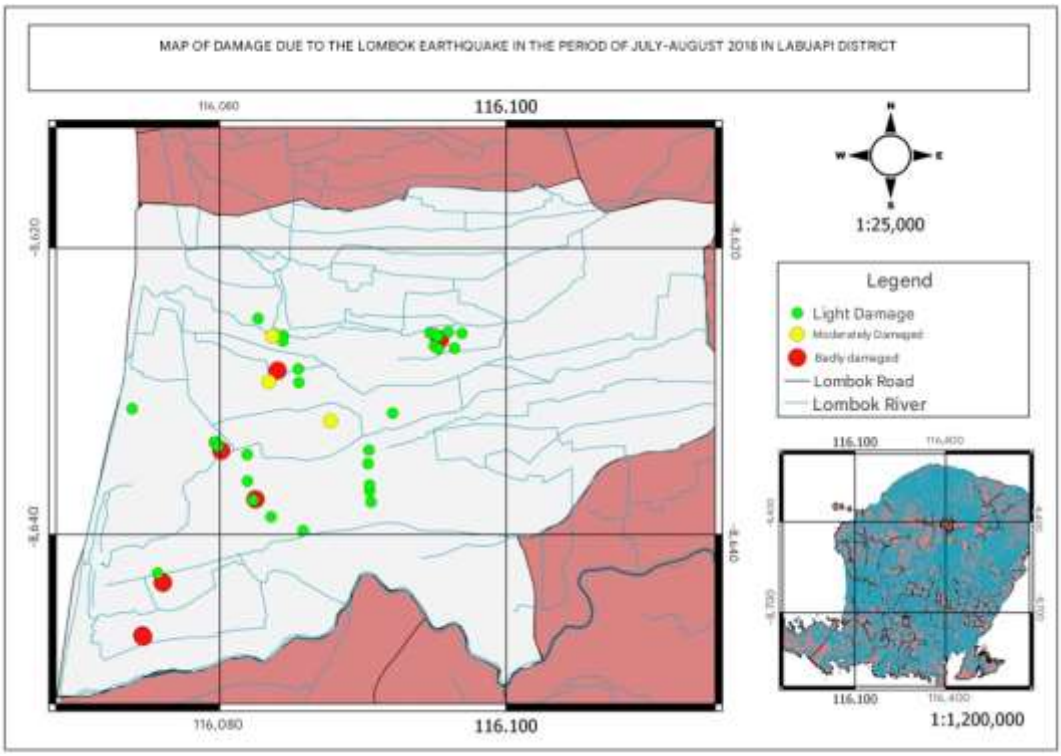

Figure 1. Map of Earthquake Damage in July-August 2018 in Labuapi District

This study aims to determine the characteristics of local site effects based on the dominant frequency value, Vs30, amplification, seismic vulnerability index (Kg), and Peak Ground Acceleration (PGA) value in Labuapi District, West Lombok Regency.

2. Method

2.1 Place and Time of Research

This research will be conducted in Labuapi District, West Lombok Regency. While the location of data processing is carried out at the BMKG Mataram office and the Basic Physics Laboratory, Faculty of Mathematics and Natural Sciences. The research was conducted from March to November 2019. Where the earthquake time used was the earthquake of August 5, 2018, and the data processing time was carried out in September 2019. The research location is shown in Figure 2.

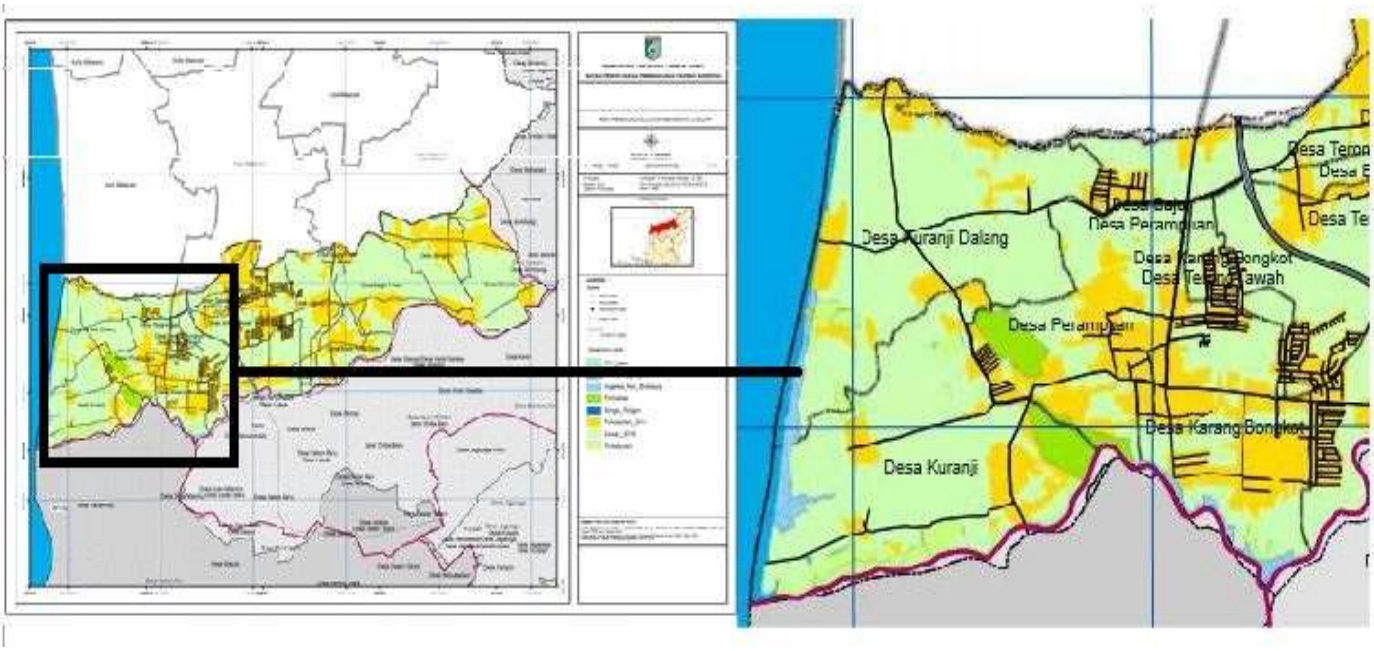

Figure 2. Research Location Map

2.2 Research Tools and Materials

The tools and materials used in this research are:

a) One set of Seismograph type TDS – 303S.
b) One GPSMAP type 60CSx as a coordinate determinant.
c) One compass as a wind direction determinant.
d) One laptop equipped with Google Earth, DataPro, Geopsy, Ms. Excel, Surfer, Qgis software

2.3 Data Collection

a) Primary Data

Create a grid of planned measurement locations by determining the distance of each measurement point as in Figure 3. The number of microtremor measurements is 24 measurement points with a distance between measurement points of 500 meters.

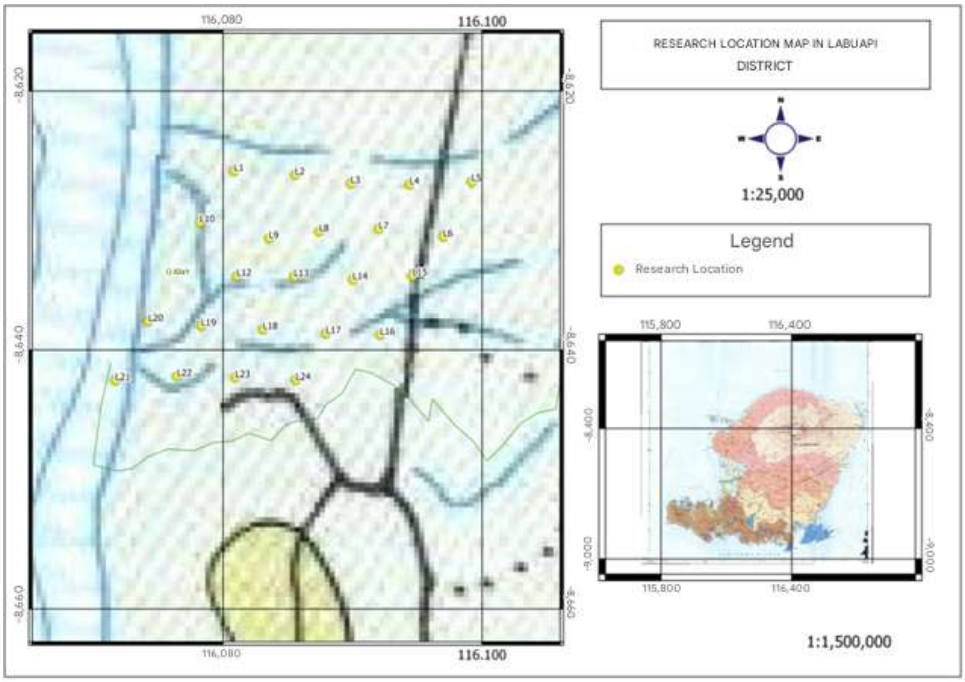

Figure 3 Measurement Points

Each measurement point was measured for 30 minutes with a sampling frequency of 100 Hz. The microtremor survey technique used refers to the SESAME European Research Project 2004 standard. Conducting data checks, if there is data that is considered not good at a certain point, then a re-measurement will be carried out.

b) Secondary Data

In this study, secondary data used in the form of earthquake catalogs and Vs30 data. For data retrieval, the earthquake catalog consists of: epicenter coordinates, earthquake time, depth, and magnitude. This catalog data comes from the Meteorology, Climatology and Geophysics Agency (BMKG). Meanwhile, the Vs30 value can be obtained from the USGS (United States Geological Survey) which is accessed [9].

2.4 Data Processing

The measurement data were initially obtained as time-domain vibration records in the TRC format. These data were subsequently converted into Mini-SEED format using the DataPro software to enable further processing with Geopsy. The output generated by Geopsy consists of the average microtremor spectrum, as illustrated in Figure 4. From this spectrum, the dominant frequency value (f_0) and the peak amplitude of the microtremor spectrum (A) at the measurement location can be identified. Based on the dominant frequency and amplification values, the seismic vulnerability index can then be determined using Equation (3).

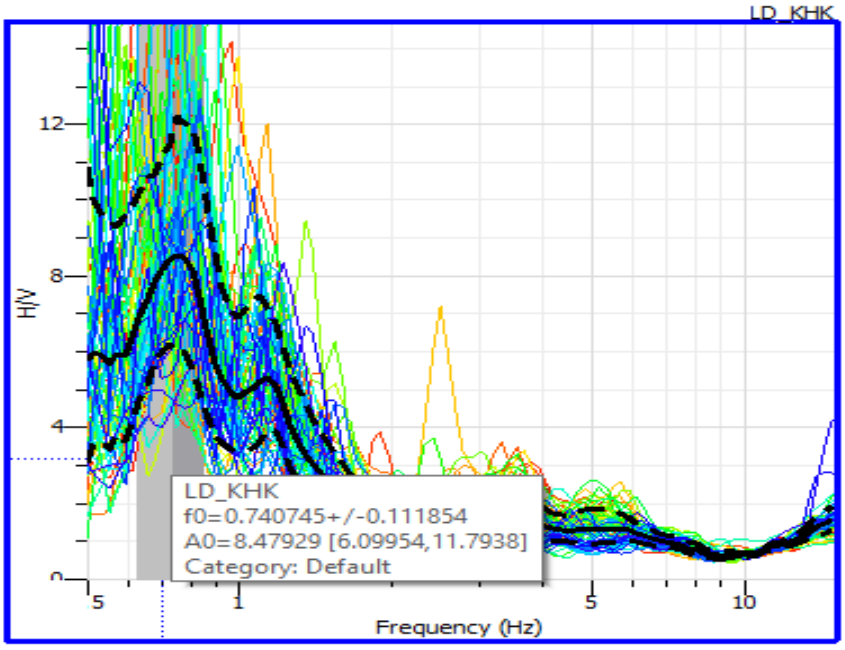

Figure 4. HVSR Graph Output from Geopsy Software

To calculate the PGA value obtained from the BMKG earthquake catalog. Before calculating this value, the dominant period value obtained from previous microtremor measurements that produce dominant frequency values is also required. After obtaining the dominant period value, the PGA value can be calculated using the empirical equation of the Kanai Method [10]. Then, from the five parameters obtained in the form of dominant frequency values (f0), amplification (A0), Vs30, seismic vulnerability index (Kg), and Peak Ground Acceleration (PGA) values, their distribution can be made using Surfer 10.

3. Result and Discussion

4.1 Damage Map

The results of the survey that has been conducted, it is known that the impact of damage felt by residents at the research location is at the level of light damage to heavy damage [11]. Areas with light damage are marked with green circles, while areas with moderate damage are marked with yellow circles, and areas with heavy damage are marked with red circles in Figure 5.

4.2 *Dominant Frequency*

The results of microtremor data processing at twenty-four measurement points in four villages in Labuapi District, obtained frequency values ranging from 0.6 - 12 Hz. Referring to the classification of soil based on the dominant microtremor frequency value according to Kanai in Di Matteo et al. [12] areas with low frequencies, namely 0.5 Hz - 4.5 Hz are indicated by blue and green zones on Map 5.2, including soil types III and IV which are composed of alluvial rocks formed from delta sedimentation, top soil, mud. Areas with this frequency have thick sediment thickness on their surfaces with a depth of > 5 meters.

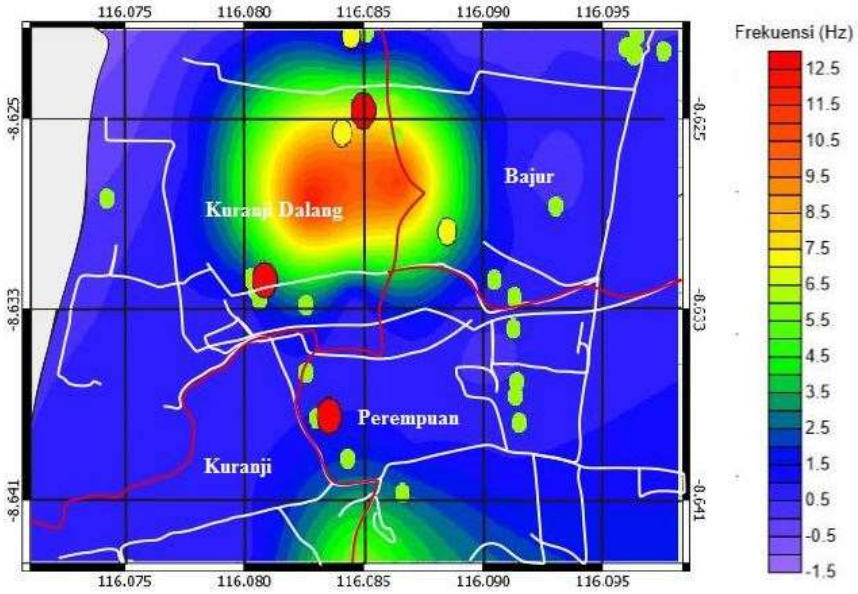

Figure 4. Contour Map of Dominant Frequency Values in the Research Area

Furthermore, areas with medium frequencies with a range of 4.5 Hz - 8.5 Hz are marked in yellow (Figure 4) are soils composed of alluvial rocks and consist of gravelly sand, hard soil sand, clay, and have a surface sediment thickness of between 5 - 10 meters. Then the area with a high frequency of 8.5 Hz – 12.5 Hz, shown in red (Figure 4) is an area composed of tertiary rocks consisting of hard sandy, gravel, and others. Areas with this frequency have a very thin surface sediment thickness, and are dominated by hard rocks [13].

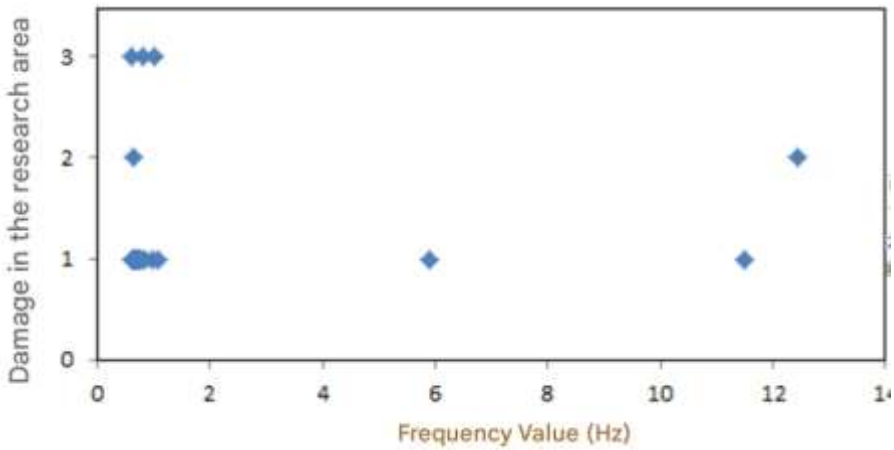

Figure 5. Graph of the Relationship between Frequency and Damage

Figure 5 shows the relationship between frequency values and damage in the research area. Where from the graph it can be seen that areas with low frequencies are dominated by light to heavy damage levels. However, from the image it is also found that areas with high frequencies have light and moderate damage. This graph shows that in addition to being influenced by geological conditions, the damaged area is also influenced by the structure of the building itself. Because areas with high frequencies indicate that the area has a very thin layer of sediment, so the impact of the damage caused is light.

4.3 Amplification Factor

Figure 6 shows that the range of amplification values in the research area ranges from 1.78 to 11.41 times. From the figure, areas with low to high amplification can be identified.

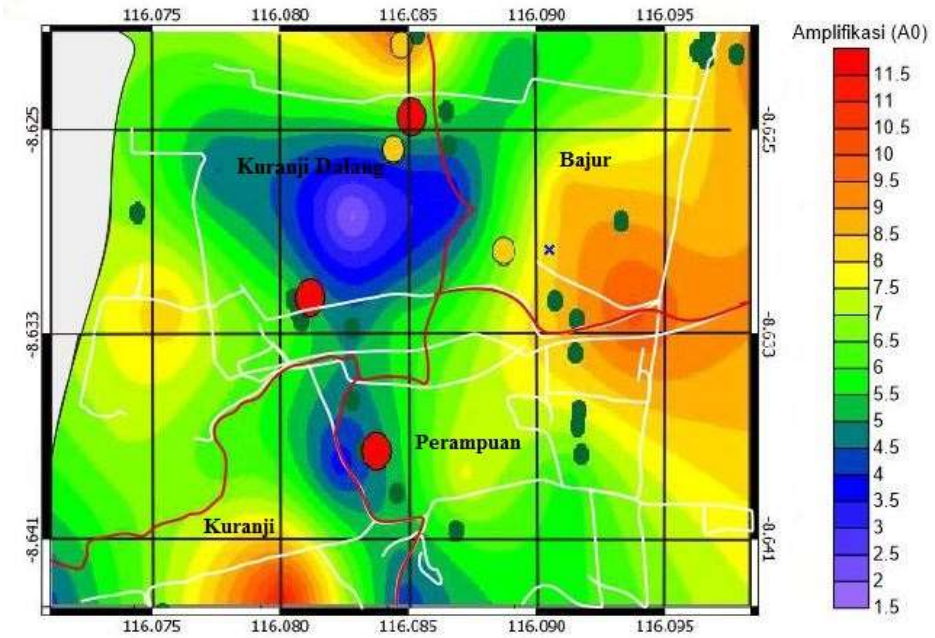

Figure 6. Contour Map of Amplification Values in the Research Area

Where in Figure 7 shows areas with low amplification marked in purple and blue with a value range of 1.5 to 4.5 times. For areas with moderate amplification, they are marked in green and yellow with a value range of 5.5 to 8.5 times. While areas with high amplification are marked in red with a value range of 9.5 to 12.5 times.

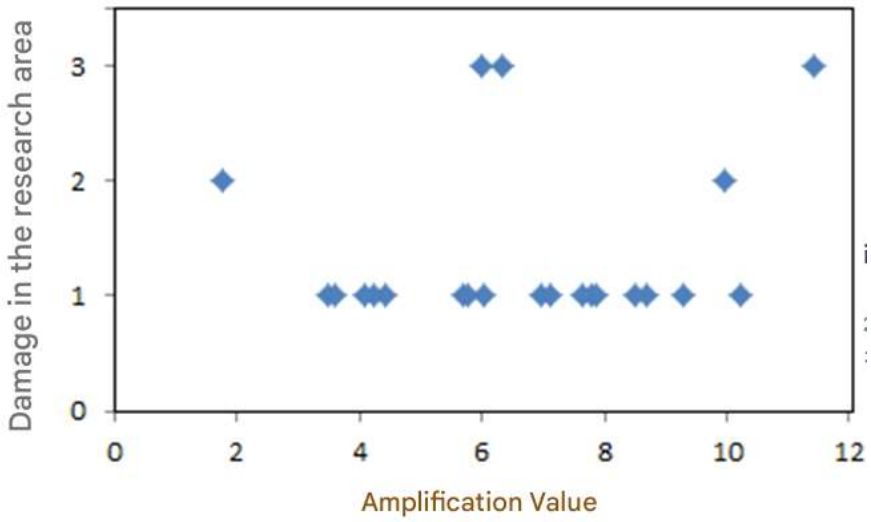

Figure 7. Graph of the Relationship between Amplification and Damage

The relationship between amplification and damage in Figure 7 shows that more damage is found in medium and high amplification which is dominated by light to heavy damage. While areas with low amplification are dominated by light and moderate damage. From this graph, it can be seen that the amplification value of each point is different. This is because the amplification value can increase if the rock has undergone deformation (weathering) which changes the physical properties of the rock. In other words, in the same rock the amplification value will vary according to the level of deformation in the rock.

4.4 PGA (Peak Ground Acceleration)

The contour map of the distribution of ground vibration acceleration values can be seen in Figure 8, where the range of ground vibration acceleration values is between 169 m/s^2-

764 m/s^2. Where the low PGA value is marked with the purple and blue zones in Figure 8 with a range of 166 cm/s^2-365 cm/s^2. For medium PGA values, they have a range of 366 cm/s^2-565 cm/s2, marked with green and yellow zones. While the high PGA value is indicated by the red color with a range of 566 cm/s^2-765 cm/s^2.

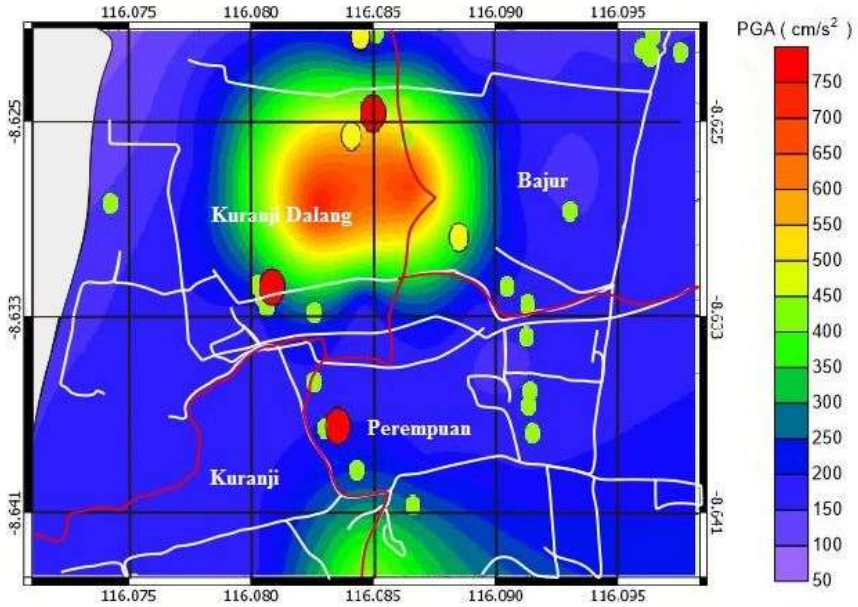

Figure 8. Contour Map of PGA Values in the Research Area

Damage and collapse of buildings due to earthquakes occur because the building is unable to anticipate the ground motion vibrations (PGA) caused by it [14]. The magnitude of ground vibrations due to earthquakes is influenced by three things, the earthquake source (source), the wave propagation path (path), and the influence of local soil conditions (site).

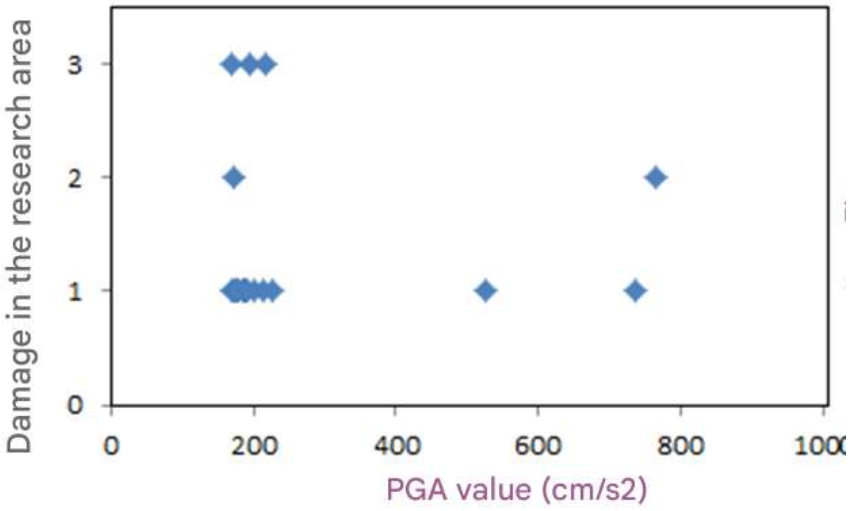

Figure 9. Graph of the Relationship between PGA and Damage

The greater the earthquake magnitude and the closer to the earthquake source, the greater the PGA value. In addition, the magnitude of the PGA value is also influenced by the magnitude of the dominant period value at the microtremor measurement point. So that Figure 9 illustrates the same relationship as the dominant frequency (Figure 4) because of the influence of the period value which is inversely proportional to the dominant frequency [15]. Thinner sediment layers have high frequency values, which means they have a small dominant period, so that in this area a higher PGA value is obtained and if an earthquake occurs the location will experience faster shaking but in a shorter duration. Meanwhile,

thicker sediment layers will cause lower PGA, with shaking that is felt slower but stronger (amplified) and lasts for a longer duration and can cause severe damage to buildings.

4.5 Seismic Vulnerability Index (Kg)

The value of the seismic vulnerability index is related to the level of vulnerability of an area to the threat of earthquake risk [16]. The greater the value of the seismic vulnerability index in an area, the greater the level of earthquake risk to damage due to earthquakes.

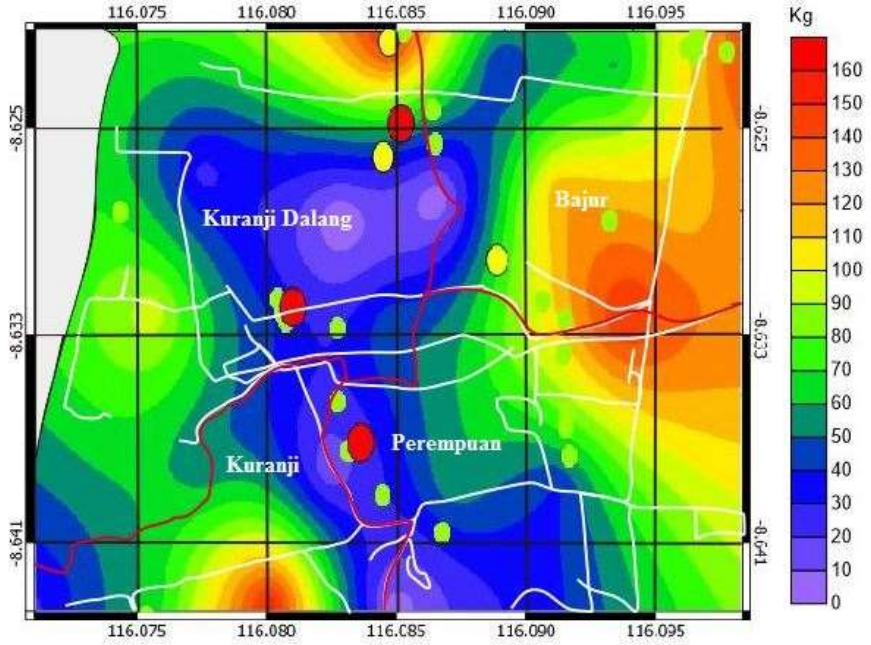

Figure 10. Contour Map of Seismic Vulnerability Index Values in the Research Area

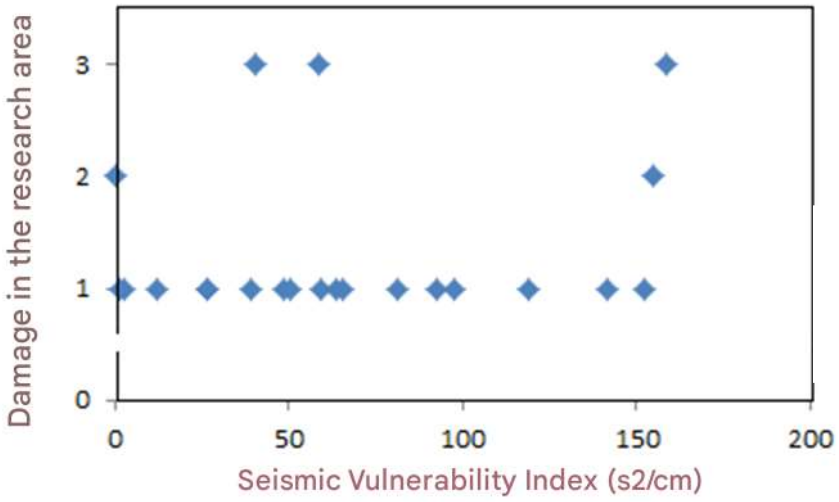

Figure 11. Graph of the Relationship between Seismic Vulnerability Index and Damage

Based on Figure 10, the value of the seismic vulnerability index ranges from 0.25 - 158. Areas with a low seismic vulnerability index are indicated by the purple-blue zone with a range of 0 - 51. While areas with a moderate vulnerability index are indicated by green-yellow with a range of 52 – 103, And areas with a range of 104 - 155 are areas with a high vulnerability index marked in red. The value of the seismic vulnerability index obtained at each measurement point varies even though the area has the same geology. Based on Figure 11, the seismic vulnerability index of each damage point at the research location can be seen. Where areas with a low seismic vulnerability index have light to heavy damage levels. While areas with a moderate seismic vulnerability index are dominated by light damage levels [17]. And for areas with a high seismic vulnerability index, they have light and moderate damage levels. The value of this seismic vulnerability index is influenced by the

amplification and frequency factors of the research location. From this graph, it is known that more damage is in the low seismic vulnerability index zone [18].

4.6 Vs30

Figure 12 shows that the research area is an area that has a low Vs30 value with a range of 241 m/s – 265 m/s. Where areas with low Vs30 indicate that the area is composed of soft sediment. This Vs30 data was obtained from USGS, where based on USGS data, the range of Vs30 values in four villages in Labuapi District ranges from 240 m/s – 300 m/s. Where based on Table 4 site class classification based on Vs30, it is found that the four villages in Labuapi District are included in soil class D which is medium soil [19].

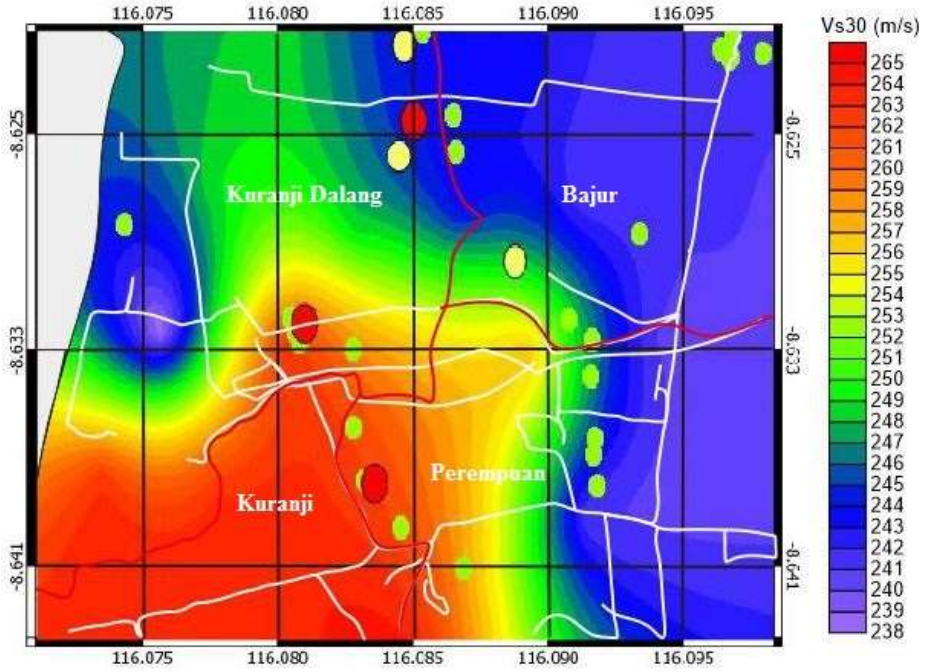

Figure 12. Contour Map of Vs30 Values in the Research Area

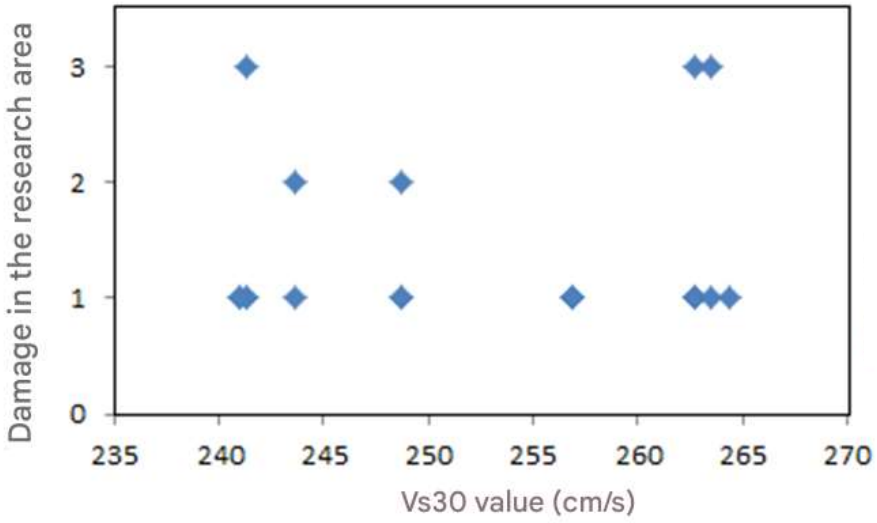

Figure 13. Graph of the Relationship between Vs30 and Damage

Referring to the geology of the area Tajidan et al. [20], the area in Labuapi sub-district is composed of alluvium deposits, where alluvium deposits are deposits consisting of river, beach and swamp deposits. Which are composed of sandy silt - clayey silt, loose sand, gravel is very soft - dense and has medium - high porosity. Alluvium deposits are also known as soft deposits, where soft deposits have low velocity values. So that 4 villages in Labuapi sub-district have low wave velocity values up to a depth of 30 meters (Vs30).

4. Conclusions

Based on the research that has been done, it can be concluded that the results of data processing show that the layer structure in the research area has a relatively low frequency value of 0.6 Hz - 12 Hz, with a variation in the amplification factor between 1 - 11. The variation in the seismic vulnerability index value (Kg) ranges from 0.25 - 150, which illustrates that the research area has a relatively high level of vulnerability. The Vs30 value in the research area is relatively low, namely 240 m / s - 262 m / s, while the PGA value obtained ranges from 160 cm / s2 - 760 cm / s2. By looking at the results of the correlation between measurement data and damage data, it shows that the damage in the research area is more dominantly influenced by the building structure.

5. Acknowledgement

The author would like to thank his colleagues at BMKG (I Gusti Satria Bunaga, S.Tr, Ricko Kardoso, S.Tr, and Rian Mahendra Taruna, S.Tr, M.T) who have assisted during the data collection process and helped with data processing. As well as colleagues at the Campus (M. Ardi Jukhairdiman, Qurrota A'yun, Happyzhatul Mar'ah, Yuyun Ustina, Rima Yudiana, Romi Mi'rajullaily, Rika Aprianti and Rita Wahyuni) who have taken the time to help with data collection.

6. References

[1] M. Wibowo, W. Kongko, W. Hendriyono, and S. Karima, 'Tsunami Hazard Potential Modeling as Tourism Development Considerations in the North of Lombok Strait', *IOP Conf. Ser.: Earth Environ. Sci.*, vol. 832, no. 1, p. 012047, Jul. 2021, doi: 10.1088/1755-1315/832/1/012047.

[2] A. T. Sasmi *et al.*, 'Shear wave splitting of the 2018 Lombok earthquake aftershock area, Indonesia', *Geosci. Lett.*, vol. 10, no. 1, p. 7, Jan. 2023, doi: 10.1186/s40562-022-00258-3.

[3] P. A. Wahyudi, P. Purwanto, and T. T. Putranto, 'Distribution of land stability based on standard penetration value (SPT) with various depth in Semarang city, Indonesia', *IOP Conf. Ser.: Earth Environ. Sci.*, vol. 832, no. 1, p. 012007, Jul. 2021, doi: 10.1088/1755-1315/832/1/012007.

[4] R. S. Salsabila, T. Yudistira, and A. Tohari, 'Mapping of Soil Dynamic Response of Palu City Based on Horizontal to Vertical Spectral Ratio (HVSR) Method', *IOP Conf. Ser.: Earth Environ. Sci.*, vol. 1288, no. 1, p. 012019, Dec. 2023, doi: 10.1088/1755-1315/1288/1/012019.

[5] O. Akin and N. Sayil, 'Soil Characterization in Landslide-Prone Areas Using Ground Shear Strain Based on Active and Passive Source Surface Wave Methods', *Pure Appl. Geophys.*, Mar. 2025, doi: 10.1007/s00024-025-03696-0.

[6] A. Brunelli *et al.*, 'Numerical simulation of the seismic response and soil–structure interaction for a monitored masonry school building damaged by the 2016 Central Italy earthquake', *Bull Earthquake Eng*, vol. 19, no. 2, pp. 1181–1211, Jan. 2021, doi: 10.1007/s10518-020-00980-3.

[7] Y. Jin, S. Jeong, M. Moon, and D. Kim, 'Analysis of the Dynamic Behavior of Multi-Layered Soil Grounds', *Applied Sciences*, vol. 14, no. 12, Art. no. 12, Jan. 2024, doi: 10.3390/app14125256.

[8] M. Gxasheka, C. S. Gajana, and P. Dlamini, 'The role of topographic and soil factors on woody plant encroachment in mountainous rangelands: A mini literature review', *Heliyon*, vol. 9, no. 10, Oct. 2023, doi: 10.1016/j.heliyon.2023.e20615.

[9] J. Wang and T. Tanimoto, 'Estimation of Vs30 at the EarthScope Transportable Array Stations by Inversion of Low-Frequency Seismic Noise', *Journal of Geophysical Research: Solid Earth*, vol. 127, no. 4, p. e2021JB023469, 2022, doi: 10.1029/2021JB023469.

[10] I. U. Meidji, S. Mulyati, N. R. Janat, H. Jayadi, and Asrafil, 'Determination of earthquake prone zones at university of tadulako based on dominant periods and peak ground acceleration (PGA)', *IOP Conf. Ser.: Mater. Sci. Eng.*, vol. 1212, no. 1, p. 012037, Jan. 2022, doi: 10.1088/1757-899X/1212/1/012037.

[11] B. Yön, İ. Ö. Dedeoğlu, M. Yetkin, H. Erkek, and Y. Calayır, 'Evaluation of the seismic response of reinforced concrete buildings in the light of lessons learned from the February 6, 2023, Kahramanmaraş, Türkiye earthquake sequences', *Nat Hazards*, vol. 121, no. 1, pp. 873–909, Jan. 2025, doi: 10.1007/s11069-024-06859-9.

[12] S. Di Matteo, U. Villante, N. Viall, L. Kepko, and S. Wallace, 'On Differentiating Multiple Types of ULF Magnetospheric Waves in Response to Solar Wind Periodic Density Structures', *Journal of Geophysical Research: Space Physics*, vol. 127, no. 3, p. e2021JA030144, 2022, doi: 10.1029/2021JA030144.

[13] M. N. Irham, M. Zainuri, G. Yuliyanto, and A. Wirasatriya, 'Measurement of ground response of Semarang coastal region risk of earthquakes by Horizontal To Vertical Spectral Ratio (HVSR) microtremor method', *J. Phys.: Conf. Ser.*, vol. 1943, no. 1, p. 012033, Jul. 2021, doi: 10.1088/1742-6596/1943/1/012033.

[14] J. Chen, H. Tang, J. Ge, and Y. Pan, 'Rapid Assessment of Building Damage Using Multi-Source Data: A Case Study of April 2015 Nepal Earthquake', *Remote Sensing*, vol. 14, no. 6, Art. no. 6, Jan. 2022, doi: 10.3390/rs14061358.

[15] J. Bisquert and M. Janssen, 'From Frequency Domain to Time Transient Methods for Halide Perovskite Solar Cells: The Connections of IMPS, IMVS, TPC, and TPV', *J. Phys. Chem. Lett.*, vol. 12, no. 33, pp. 7964–7971, Aug. 2021, doi: 10.1021/acs.jpclett.1c02065.

[16] J. Han, A. S. Nur, M. Syifa, M. Ha, C.-W. Lee, and K.-Y. Lee, 'Improvement of Earthquake Risk Awareness and Seismic Literacy of Korean Citizens through Earthquake Vulnerability Map from the 2017 Pohang Earthquake, South Korea', *Remote Sensing*, vol. 13, no. 7, Art. no. 7, Jan. 2021, doi: 10.3390/rs13071365.

[17] A. Masi, S. Lagomarsino, M. Dolce, V. Manfredi, and D. Ottonelli, 'Towards the updated Italian seismic risk assessment: exposure and vulnerability modelling', *Bull Earthquake Eng*, vol. 19, no. 8, pp. 3253–3286, Jun. 2021, doi: 10.1007/s10518-021-01065-5.

[18] A. Doğan, M. Başeğmez, and C. C. Aydın, 'Assessment of the seismic vulnerability in an urban area with the integration of machine learning methods and GIS', *Nat Hazards*, Mar. 2025, doi: 10.1007/s11069-025-07185-4.

[19] A. Nikmatullah, G. G. Samudra, K. Zawani, K. Muslim, I. Nairfana, and M. Sarjan, 'Foliar Organic Fertilizer Enhanced Growth, Yield and Carotenoid Content of Carrot Plants (Daucus carota L.) Cultivated in the Lowland', *IOP Conf. Ser.: Earth Environ. Sci.*, vol. 913, no. 1, p. 012019, Nov. 2021, doi: 10.1088/1755-1315/913/1/012019.

[20] T. Tajidan, H. Halil, M. Siddik, S. Sofwan, and D. R. Yunidiya, 'A single control area policy as a threat to food security in West Lombok Regency', *IOP Conf. Ser.: Earth Environ. Sci.*, vol. 1253, no. 1, p. 012063, Oct. 2023, doi: 10.1088/1755-1315/1253/1/012063.